Low order models representing realizations of turbulence

By EDWARD N. LORENZ

Department of Meteorology, Massachusetts Institute of Technology

The equations governing two-dimensional turbulence are written as an infinite system of ordinary differential equations, in which the dependent variables are the coefficients in the expansion of the vorticity field in a double Fourier series. The variables are sorted into sets which correspond to consecutive bands in the wavenumber spectrum; within each set it is supposed that the separate variables will exhibit statistically similar behaviour. A low order model is then constructed by retaining only a few variables within each set. Multiplicative factors are introduced into the equations to compensate for the reduced number of terms in the summations. Like the original equations, the low order equations conserve kinetic energy and enstrophy, apart from the effects of external forcing and viscous dissipation.

A special case is presented in which the bands are half octaves and there is effectively only one dependent variable per set. Solutions of these equations are compared with conventional numerical simulations of turbulence, and agree reasonably well, although the nonlinear effects are somewhat underestimated.

1. Introduction

Turbulence, or more specifically an ensemble of time-dependent fields of turbulent motion, constitutes a *process*. A particular member of any such ensemble constitutes a *realization* of the process. A characteristic feature of turbulent motion is the simultaneous presence of eddies of many different sizes. This feature renders it impossible, when treating turbulence by mathematical techniques, to represent a realization by a relatively simple analytic function. By contrast, certain statistical properties of a turbulent process, such as the energy spectrum, often lack the irregularity of individual realizations and, if not expressible by the more familiar analytic functions, may at least be represented by rather simple smooth curves. Consequently many theoreticians concerned with turbulence have confined their attention to ensemble statistics, as a means of finding order within apparent chaos.

If we begin with the Navier–Stokes equations or some other equations which are assumed to govern the flow, we may in principle use either of two approaches in seeking the statistical properties. We may obtain a number of particular solutions, each representing a realization, and then compile statistics from them. Alternatively we may derive new equations whose unknowns are statistical properties and then solve the new equations.

The former approach is rendered extremely cumbersome by the presence of

motions of many scales. If the relevant motions cover s octaves of the spectrum, at least 2^{ns} numbers are needed to describe a realization of n-dimensional turbulence at a single instant ($n = 2$ or 3). Two-dimensional turbulence spanning twelve octaves, or three-dimensional turbulence spanning eight, is therefore well beyond the scope of today's most powerful computers, yet studies encompassing fewer octaves often cannot promise realistic results. In the atmosphere, for example, which is a highly turbulent system, extratropical cyclones and cumulus clouds, both of which exert considerable influence upon the total motion, differ by about ten octaves in scale.

In the latter approach each pertinent statistical property can often be represented by relatively few numbers, thanks to its rather smooth behaviour. The numerical description becomes particularly concise when the turbulence is homogeneous and isotropic. The main difficulty stems from the nonlinearity of the governing equations, which inevitably causes any finite system of derived equations with statistical properties as unknowns to contain more unknowns than equations. To increase the number of equations to the number of unknowns it is necessary to introduce some *closure* approximation. One of the best known of these is the quasinormal approximation, originally introduced by Millionshtchikov (1941), expressing fourth-degree statistical properties in terms of statistics of lower degree. More refined closure schemes include the original direct-interaction approximation of Kraichnan (1959). These and other schemes have recently been reviewed by Orszag (1970).

The basis for accepting or rejecting a closure approximation has frequently been not any *a priori* demonstration of suitability, but rather the results which have eventually been obtained when the scheme has been put to use. The quasinormal approximation, for example, became discredited after Ogura (1963) demonstrated by numerical integration that it would lead to the physically impossible occurrence of negative kinetic energy in certain bands of the spectrum. Thus, when one obtains a result using some particular closure scheme, the question always remains as to the extent to which the result has been deduced and the extent to which it has been implicitly presupposed in selecting the scheme.

To eliminate the need for closure approximations one may return to the former approach, and deal with realizations. This procedure is indeed becoming more common, with the increasing availability of more powerful computers. Lilly (1969), for example, has represented a two-dimensional turbulent field by the values of a stream function at a grid of 64×64 points, and has obtained flow patterns which seem fairly realistic. However, his six-octave span falls far short of the ten or more octaves which one often wishes to cover.

It is the purpose of this study to devise a means for representing *realizations* of turbulence with relatively few numbers while still retaining many octaves of the spectrum and to establish systems of equations governing these representations. The speed and capacity of present-day computers will then cease to be a limiting factor. Needless to say, the representations will have to be unrealistic in some respect other than the total spectral range.

In brief, we first represent a realization by a multiple Fourier series in space whose coefficients are functions of time alone. These coefficients become the

dependent variables in an infinite system of ordinary differential equations, derived from the original governing equations. We next divide the wavenumber spectrum into relatively narrow bands (e.g. half octaves). We then discard most of the variables corresponding to each band, retaining only a small number whose statistical behaviour is supposed to be representative of the behaviour of all the variables in that band. We attempt to compensate for the reduced number of terms in each equation by introducing suitable multiplicative factors. The author (1971*b*) has recently proposed that a scheme of this sort could be of value in investigating the *predictability* of turbulence, and has described some of the ingredients of a particular scheme. Although we shall deal only with two-dimensional turbulence in this study, there is no obvious reason why a similar scheme could not be used in three dimensions.

2. The basic equations

We shall first introduce the basic equations, from which the special equations of this study will be derived. Since the same basic equations have appeared in numerous works, we shall simply state them, without detailed derivations.

Consider the mechanically forced motion of a two-dimensional homogeneous incompressible viscous fluid of infinite horizontal extent. Such motion may be expressed in terms of the stream function ψ or the vorticity $\nabla^2\psi$, and the governing equation may be written as

$$\frac{\partial}{\partial t}\nabla^2\psi = -\nabla\psi \times \nabla(\nabla^2\psi) + \nu\nabla^4\psi + F, \tag{1}$$

where t is time, ν is the coefficient of kinematic viscosity and F is an external forcing function, which will serve to maintain the motion against the effects of viscosity. We use two-dimensional vector notation; ∇ is the horizontal differential operator and the cross product is a scalar, which would be denoted by the vertical component of the cross product in three-dimensional notation.

Let x and y denote distances in mutually perpendicular directions and let the motion be periodic in both the x and y directions, with a fundamental period $2\pi D$, where D is a large distance. The vorticity may then be expressed as the double Fourier series

$$\nabla^2\psi = \sum_{\mathbf{J}} X_{\mathbf{J}} \exp(iD^{-1}\mathbf{J}.\mathbf{r}), \tag{2}$$

where $\mathbf{r}$ is the vector whose components are x and y, and the summation runs over all vectors $\mathbf{J}$ whose components J_x and J_y are both integers. It follows that

$$\psi = -D^2 \sum_{\mathbf{J}} J^{-2} X_{\mathbf{J}} \exp(iD^{-1}\mathbf{J}.\mathbf{r}), \tag{3}$$

where J denotes the magnitude of $\mathbf{J}$. We shall refer to J and $\mathbf{J}$ as the wavenumber and the wave vector of $X_{\mathbf{J}}$. The physical necessity for ψ and $\nabla^2\psi$ to be real demands that

$$X_{-\mathbf{J}} = X_{\mathbf{J}}^*, \tag{4}$$

where the asterisk denotes the complex conjugate. We may likewise let

$$F = \sum_{\mathbf{J}} F_{\mathbf{J}} \exp{(iD^{-1}\mathbf{J}.\mathbf{r})}, \tag{5}$$

where

$$F_{-\mathbf{J}} = F_{\mathbf{J}}^{*}. \tag{6}$$

Upon substituting (2) and (5) into the linear terms in (1), and the complex conjugates of (2) and (3) into the nonlinear term, we obtain the spectral form of the governing equation:

$$\frac{d}{dt}X_{\mathbf{J}} = \sum_{\mathbf{K},\mathbf{L}} C_{\mathbf{JKL}}X_{\mathbf{K}}^{*}X_{\mathbf{L}}^{*} - \nu D^{-2}J^{2}X_{\mathbf{J}} + F_{\mathbf{J}}, \tag{7}$$

where the interaction coefficient $C_{\mathbf{JKL}}$ is given by

$$C_{\mathbf{JKL}} = \begin{cases} -\tfrac{1}{2}(K^{-2}-L^{-2})\,\mathbf{K}\times\mathbf{L} & \text{if} \quad \mathbf{J}+\mathbf{K}+\mathbf{L} = 0, \\ 0 & \text{if} \quad \mathbf{J}+\mathbf{K}+\mathbf{L} \neq 0. \end{cases} \tag{8}$$

The summation in (7) is written redundantly, i.e. terms containing $X_{\mathbf{K}}^{*}X_{\mathbf{L}}^{*}$ and $X_{\mathbf{L}}^{*}X_{\mathbf{K}}^{*}$ are added together.

From (7) and (8) it follows that if a term containing $X_{\mathbf{K}}^{*}X_{\mathbf{L}}^{*}$ appears with a non-vanishing coefficient in the equation governing $X_{\mathbf{J}}$, terms containing $X_{\mathbf{L}}^{*}X_{\mathbf{J}}^{*}$ and $X_{\mathbf{J}}^{*}X_{\mathbf{K}}^{*}$ generally appear in the equations governing $X_{\mathbf{K}}$ and $X_{\mathbf{L}}$ respectively. Equation (7) thus depicts the evolution of the field of motion as consisting, apart from the effects of forcing and viscosity, of a collection of *interactions* of triples of wave vectors $(\mathbf{J}, \mathbf{K}, \mathbf{L})$ whose sum is zero, or, alternatively, interactions of triples of variables $(X_{\mathbf{J}}, X_{\mathbf{K}}, X_{\mathbf{L}})$.

An alternative form of (8) is

$$C_{\mathbf{JKL}} = \epsilon_{\mathbf{JKL}}(K^{-2}-L^{-2})\,A(J,K,L), \tag{9}$$

where

$$A(J,K,L) = \tfrac{1}{4}[(J+K+L)\,(-J+K+L)\,(J-K+L)\,(J+K-L)]^{\frac{1}{2}} \tag{10}$$

is the area of a triangle in wave-vector space with sides of lengths J, K and L, and

$$\epsilon_{\mathbf{JKL}} = \begin{cases} 1 & \text{if} \quad \mathbf{J}+\mathbf{K}+\mathbf{L} = 0 \quad \text{and} \quad \mathbf{K}\times\mathbf{L} < 0, \\ 0 & \text{if} \quad \mathbf{J}+\mathbf{K}+\mathbf{L} \neq 0 \quad \text{or} \quad \mathbf{K}\times\mathbf{L} = 0, \\ -1 & \text{if} \quad \mathbf{J}+\mathbf{K}+\mathbf{L} = 0 \quad \text{and} \quad \mathbf{K}\times\mathbf{L} > 0. \end{cases} \tag{11}$$

It is evident that $\epsilon_{\mathbf{JKL}}$ is unaltered by a cyclic permutation of the indices, while a transposition changes it sign. It then follows readily from (9) that

$$C_{\mathbf{JKL}} = C_{\mathbf{JLK}}, \tag{12}$$

$$C_{\mathbf{JKL}} + C_{\mathbf{KLJ}} + C_{\mathbf{LJK}} = 0, \tag{13}$$

$$J^{-2}C_{\mathbf{JKL}} + K^{-2}C_{\mathbf{KLJ}} + L^{-2}C_{\mathbf{LJK}} = 0. \tag{14}$$

The principal advantage of (9) over (8) is that, except for sign, it expresses $C_{\mathbf{JKL}}$ in terms of the (scalar) wavenumbers of the interacting variables.

The specific kinetic energy E and the enstrophy V are given by

$$E = \overline{\tfrac{1}{2}\nabla\psi.\nabla\psi}, \tag{15}$$

$$V = \overline{\tfrac{1}{2}(\nabla^{2}\psi)^{2}}, \tag{16}$$

where the bar denotes an area average. In spectral form (15) and (16) become

$$E = \tfrac{1}{2}D^2 \sum_{\mathbf{J}} J^{-2} X_{\mathbf{J}} X_{\mathbf{J}}^*, \tag{17}$$

$$V = \tfrac{1}{2} \sum_{\mathbf{J}} X_{\mathbf{J}} X_{\mathbf{J}}^*. \tag{18}$$

Here also the summations are written redundantly, i.e. for a given $\mathbf{J}$, terms containing $X_{\mathbf{J}} X_{\mathbf{J}}^*$ and $X_{-\mathbf{J}} X_{-\mathbf{J}}^*$ (i.e. $X_{\mathbf{J}}^* X_{\mathbf{J}}$) are added together.

It is well known that in the absence of external forcing and viscous dissipation equation (1), and hence (7), conserves both E and V. However, it is evident from (13) and (14) that in addition each interaction among three vectors $\mathbf{J}$, $\mathbf{K}$ and $\mathbf{L}$, together with the assured interaction among the vectors $-\mathbf{J}$, $-\mathbf{K}$ and $-\mathbf{L}$, *individually* conserves E and V. The advantages of using wave-vector space in dealing with two-dimensional turbulence stem largely from this familiar result.

3. Formulation of the low order equations

As a first step in developing a low order model we shall divide the spectrum into bands, i.e. we shall sort the wave vectors $\mathbf{J}$ into sets S_0, S_1, ... according to their magnitudes. To do this we choose a resolution factor $\rho > 1$, and assign $\mathbf{J}$ or $X_{\mathbf{J}}$ to the set S_j if $\rho^{j-\frac{1}{2}} \leqslant J < \rho^{j+\frac{1}{2}}$. It is intended that ρ should be close enough to unity so that separate variables in the same set will represent features of comparable scale, and may be expected to exhibit similar statistical behaviour.

Equation (7) may now be rewritten as

$$\frac{d}{dt} X_{\mathbf{J}} = \sum_{k,l=0}^{\infty} \sum_{\mathbf{K},\mathbf{L}}^{S_k, S_l} C_{\mathbf{JKL}} X_{\mathbf{K}}^* X_{\mathbf{L}}^* - \nu D^{-2} J^2 X_{\mathbf{J}} + F_{\mathbf{J}}, \tag{19}$$

where the second summation runs over all wave vectors $\mathbf{K}$ and $\mathbf{L}$ belonging respectively to S_k and S_l. An important derived relation is

$$\frac{d}{dt} X_{\mathbf{J}} X_{\mathbf{J}}^* = \sum_{k,l=0}^{\infty} \sum_{\mathbf{K},\mathbf{L}}^{S_k, S_l} C_{\mathbf{JKL}} (X_{\mathbf{J}} X_{\mathbf{K}} X_{\mathbf{L}} + X_{\mathbf{J}}^* X_{\mathbf{K}}^* X_{\mathbf{L}}^*)$$
$$- 2\nu D^{-2} J^2 X_{\mathbf{J}} X_{\mathbf{J}}^* + (X_{\mathbf{J}} F_{\mathbf{J}}^* + X_{\mathbf{J}}^* F_{\mathbf{J}}). \tag{20}$$

Likewise, E and V may be rewritten as

$$E = \tfrac{1}{2}D^2 \sum_{j=0}^{\infty} \sum_{\mathbf{J}}^{S_j} J^{-2} X_{\mathbf{J}} X_{\mathbf{J}}^*, \tag{21}$$

$$V = \frac{1}{2} \sum_{j=0}^{\infty} \sum_{\mathbf{J}}^{S_j} X_{\mathbf{J}} X_{\mathbf{J}}^*. \tag{22}$$

We shall denote the number of vectors $\mathbf{J}$ contained in S_j by n_j, and the number of triples of interacting vectors $(\mathbf{J}, \mathbf{K}, \mathbf{L})$ contained respectively in S_j, S_k and S_l by q_{jkl}. In defining n_j and q_{jkl}, vectors $\mathbf{J}$ and $-\mathbf{J}$ are to be counted separately, as are triples $(\mathbf{J}, \mathbf{K}, \mathbf{L})$ and $(-\mathbf{J}, -\mathbf{K}, -\mathbf{L})$. If two sets are the same, say if $k = l$, triples $(\mathbf{J}, \mathbf{K}, \mathbf{L})$ and $(\mathbf{J}, \mathbf{L}, \mathbf{K})$ are to be counted separately unless $\mathbf{K} = \mathbf{L}$. Since q_{jkl} can exceed neither $n_k n_l$, nor $n_l n_j$, nor $n_j n_k$, we may let

$$q_{jkl} = \sigma_{jkl} (n_j n_k n_l)^{\frac{2}{3}}, \tag{23}$$

whence $\sigma_{jkl} \leqslant 1$.

Given the sets S_k and S_l, the number of terms added together in the *second* summation in (19) will differ for different variables X_J in the same set S_j, but on the average there will be $n_j^{-1}q_{jkl}$ such terms. If j, k and l are large this number may also be large. Suppose that in evaluating the second summation in (19) we accumulate these terms in a more or less random order. After we have added a relatively small number of terms together, we may be able to estimate the sum of all the terms, or perhaps at least the general magnitude of the sum, more or less as one estimates the outcome of an election after a few votes have been counted.

Accordingly, we shall introduce subsets $R_0, R_1, \ldots$ of $S_0, S_1, \ldots$. We shall denote the number of vectors $\mathbf{J}$ contained in R_j by m_j, and the number of triples of interacting vectors $(\mathbf{J}, \mathbf{K}, \mathbf{L})$ contained respectively in R_j, R_k and R_l by p_{jkl}. We may then let

$$p_{jkl} = \rho_{jkl}(m_j m_k m_l)^{\frac{2}{3}}, \tag{24}$$

whence $\rho_{jkl} \leqslant 1$. We shall also introduce the ratios

$$r_j = m_j^{-1}n_j, \tag{25}$$

$$\tau_{jkl} = \rho_{jkl}^{-1}\sigma_{jkl}. \tag{26}$$

As our principal modification, we now approximate (19) by

$$\frac{d}{dt}X_{\mathbf{J}} = a_j \sum_{k,l=0}^{\infty} b_{jkl} \sum_{\mathbf{K},\mathbf{L}}^{R_k,\,R_l} C_{\mathbf{JKL}}X_{\mathbf{K}}^* X_{\mathbf{L}}^* - \nu D^{-2}J^2 X_{\mathbf{J}} + F_{\mathbf{J}}, \tag{27}$$

where j is the index of the subset containing $\mathbf{J}$, and approximate (21) and (22) by

$$E = \tfrac{1}{2}D^2 \sum_{j=0}^{\infty} c_j \sum_{\mathbf{J}}^{R_j} J^{-2}X_{\mathbf{J}}X_{\mathbf{J}}^*, \tag{28}$$

$$V = \frac{1}{2}\sum_{j=0}^{\infty} c_j \sum_{\mathbf{J}}^{R_j} X_{\mathbf{J}}X_{\mathbf{J}}^*. \tag{29}$$

We thereby omit all reference to all wave vectors and the corresponding variables except those contained in $R_0, R_1, \ldots$. Within each subset R_j the behaviour of the retained variables is supposed to be representative of that of all the variables in S_j. The factor c_j has been introduced into (28) and (29) in an effort to compensate for the reduction in the number of terms in the second summation from n_j to m_j. Likewise the factor b_{jkl} in (27) represents an attempt to compensate for the reduction in the average number of terms in the second summation from $n_j^{-1}q_{jkl}$ to $m_j^{-1}p_{jkl}$. The additional factor a_j is included to compensate for a possible reduction in the number of terms contributing significantly to the first summation, since, given j, there may be pairs (k, l) for which there are no interacting variables in R_j, R_k and R_l, and hence an empty second summation, even though there are interacting variables in S_j, S_k and S_l. The remaining problem is to determine suitable expressions for a_j, b_{jkl} and c_j.

We cannot expect that the fluctuations of the retained variables in a particular solution of the modified equation (27) will coincide with the fluctuations of the same variables in any solution of the original equation (19), nor even that the fluctuations of E and V in two such solutions will coincide. The most that we can

ask is that some of the statistical properties of the two solutions should be the same. Our choices for a_j, b_{jkl} and c_j should therefore depend upon the manner in which we expect the separate terms in the summations in (7), (17) and (18) to combine.

We can distinguish two extreme types of behaviour. If the terms in a summation are all of one sign and thus have no tendency to cancel, we can make a good estimate of the sum of all the terms by multiplying the sum of the retained terms by the ratio of the total number of terms to the number of retained terms. If, on the other hand, terms of either sign are about equally common, we cannot readily estimate the total sum, but we can estimate the general magnitude of the total sum by multiplying the sum of the retained terms by the square-root of the above-mentioned ratio. We shall refer to the two types of behaviour as *systematic* and *random*. The possibility of somewhat intermediate behaviour should also be recognized.

We shall therefore let

$$c_j = r_j^\gamma \tag{30}$$

in (28) and (29), where we choose $\gamma = 1$ if the assumed behaviour is completely systematic, but $\gamma = \frac{1}{2}$ if it is completely random. It is doubtful that any value of γ is really appropriate for intermediate behaviour, but some value between 1 and $\frac{1}{2}$ is probably preferable to either extreme. Likewise, our *tentative* choice for b_{jkl} in (27) will be

$$b'_{jkl} = (m_j p_{jkl}^{-1} n_j^{-1} q_{jkl})^\beta = r_j^{-\beta} (r_j r_k r_l)^{\frac{2}{3}\beta} \tau_{jkl}^\beta, \tag{31}$$

where the same considerations as determine γ are to determine β. We shall temporarily leave the exponents γ and β unspecified, so that the ensuing equations will be applicable to a number of possible choices.

We also wish the modified equations to continue to conserve E and V in the absence of external forcing and viscous dissipation. According to (27), (28) and (29), this requires that

$$c_j a_j b_{jkl} J^{-2} C_{\mathbf{JKL}} + c_k a_k b_{klj} K^{-2} C_{\mathbf{KLJ}} + c_l a_l b_{ljk} L^{-2} C_{\mathbf{LJK}} = 0, \tag{32}$$

$$c_j a_j b_{jkl} C_{\mathbf{JKL}} + c_k a_k b_{klj} C_{\mathbf{KLJ}} + c_l a_l b_{ljk} C_{\mathbf{LKJ}} = 0, \tag{33}$$

for any three interacting vectors $\mathbf{J}$, $\mathbf{K}$ and $\mathbf{L}$ contained in any three sets R_j, R_k and R_l. Comparing (32) and (33) with (13) and (14), we find that

$$c_j a_j b_{jkl} = c_k a_k b_{klj} = c_l a_l b_{ljk}. \tag{34}$$

The proper choice for b_{jkl} must then depend upon the choice for a_j, whence the tentative choice (31) cannot be suitable in all cases.

We shall presently offer a procedure for choosing a_j; meanwhile we shall assume that a_j neither increases nor decreases systematically as j increases. It is evident that n_j increases as ρ^{2j} for large values of j. We shall assume that the subsets R_j have been chosen so that m_j increases as a lower power of ρ^j, whence r_j also increases as a power of ρ^j.

As a choice for b_{jkl} which does not violate (34) and yet retains the essence of the tentative choice (31), we take b'_{jkl} multiplied by a function of a_j, a_k, a_l and r_j, r_k, r_l
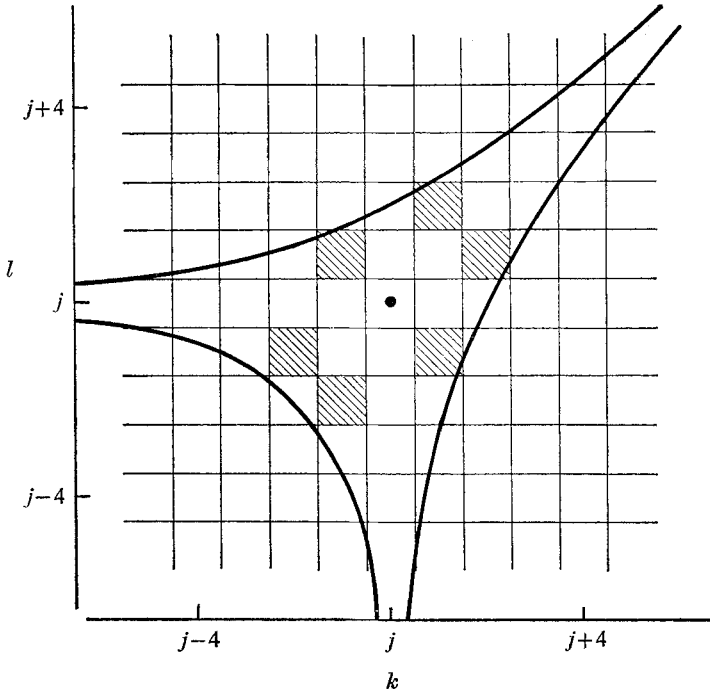
FIGURE 1. A portion of the k, l plane. $\bullet$, (j, j); ———, $K + L = J$ (lower left), $J + K = L$ (upper) and $J + L = K$ (right), where $J = \rho^j$, $K = \rho^k$, $L = \rho^l$ and $\rho = \sqrt{2}$. Small squares formed by intersecting lines are of unit area, and the co-ordinates of central points of shaded small squares are $(j-2, j-1)$, $(j-1, j-2)$, $(j-1, j+1)$, $(j+1, j-1)$, $(j+1, j+2)$ and $(j+2, j+1)$.

which neither increases nor decreases systematically as j, k and l increase together. We can do this by letting

$$b_{jkl} = (a_j^{-2} a_k a_l)^{\frac{1}{3}} (r_j^{-2} r_k r_l)^{\frac{1}{3}(\gamma - \beta)} b'_{jkl}$$
$$= a_j^{-1} r_j^{-\gamma} (a_j a_k a_l)^{\frac{1}{3}} (r_j r_k r_l)^{\frac{1}{3}(\gamma + \beta)} r_{jkl}^{\beta}. \tag{35}$$

Choosing a_j presents further problems. Whereas the separate variables within a band can be expected to exhibit somewhat similar statistical behaviour, variables in separate bands presumably cannot. Nevertheless, given j, if for some k and l the interactions in (S_j, S_k, S_l) are not represented by any interactions in (R_j, R_k, R_l), the only way in which their effects can be represented would seem to be in terms of interactions in other triples of bands.

A reasonably satisfactory procedure for choosing a_j is perhaps best described with the aid of a diagram. In figure 1 the horizontal co-ordinates are k and l, regarded as continuous variables. The central point is (j, j), where j is an integer. The horizontal and vertical lines divide the k, l plane into squares of unit area, and the co-ordinates of the centres of the squares are integers.

The equations of the heavy curves are $\rho^k + \rho^l = \rho^j$, $\rho^j + \rho^l = \rho^k$ and $\rho^j + \rho^k = \rho^l$. The region enclosed by these curves, which we shall call the *interaction region*, therefore contains the values of k and l for which none of the three quantities ρ^j, ρ^k and ρ^l exceeds the sum of the other two, and for which interacting vectors

with magnitudes ρ^j, ρ^k and ρ^l can therefore exist. Figure 1 has been drawn with $\rho = \sqrt{2}$.

The squares which intersect the interaction region are centred at those points (k, l) for which interactions in S_j, S_k and S_l exist. We shall denote the number of such squares by N'_j. The shaded squares, all of which intersect the interaction region, are centred at those points (k, l) for which at least one interaction in R_j, R_k and R_l exists. We shall denote the number of such squares by M'_j. In the particular case shown in figure 1, the squares are centred at $(j-2, j-1)$, $(j-1, j-2)$, $(j-1, j+1)$, $(j+1, j-1)$, $(j+1, j+2)$ and $(j+2, j+1)$, i.e. all the retained interactions occur among triples of vectors occupying three consecutive bands.

Although M'_j may be finite, N'_j is clearly infinite, and it is for this reason that we cannot let a_j depend simply upon the ratio N'_j/M'_j. However, under the assumption that squares lying mostly outside the interaction region represent rather few interactions compared with nearby squares lying mainly inside the interaction region, we may let a_j depend upon the ratio of the area of the interaction region to the area of the shaded portion of the interaction region.

We shall denote the latter area, which cannot exceed M'_j, by M_j. For any particular case M_j may be determined by direct measurement. Direct integration reveals that the area of the interaction region (extending to infinity in each direction) is

$$I = \tfrac{1}{2}\pi^2(\ln \rho)^{-2}. \tag{36}$$

We shall let

$$a_j = (M_j^{-1}I)^\alpha, \tag{37}$$

where the considerations which govern the choices of γ and β also govern the choice of α. In the case illustrated in figure 1, $I = 41 \cdot 1$ and $M_j = 5 \cdot 8$, whence $a_j = (7 \cdot 1)^\alpha$.

A further modification, less drastic than those already introduced, is suggested by the narrowness of the spectral bands. We replace J by ρ^j and, in evaluating c_{JKL}, we also replace K by ρ^k and L by ρ^l. If we now let

$$Y_{\mathbf{J}} = c_j^{\frac{1}{2}} X_{\mathbf{J}}, \quad G_{\mathbf{J}} = c_j^{\frac{1}{2}} F_{\mathbf{J}}, \tag{38}, (39)$$

we find that

$$E = \tfrac{1}{2}D^2 \sum_{j=0}^{\infty} \rho^{-2j} \sum_{\mathbf{J}}^{R_j} Y_{\mathbf{J}} Y_{\mathbf{J}}^*, \tag{40}$$

$$V = \frac{1}{2}\sum_{j=0}^{\infty} \sum_{\mathbf{J}}^{R_j} Y_{\mathbf{J}} Y_{\mathbf{J}}^*, \tag{41}$$

while the governing equation (19) becomes

$$\frac{d}{dt}Y_{\mathbf{J}} = \sum_{k,\,l=0}^{\infty} g_{jkl} C'_{jkl} \sum_{\mathbf{K},\,\mathbf{L}}^{R_k,\,R_l} \epsilon_{\mathbf{JKL}} Y_{\mathbf{K}}^* Y_{\mathbf{L}}^* - \nu D^{-2}\rho^{2j}Y_{\mathbf{J}} + G_{\mathbf{J}}, \tag{42}$$

where

$$C'_{jkl} = (\rho^{-2k} - \rho^{-2l})\,A(\rho^j, \rho^k, \rho^l) \tag{43}$$

is a quantity which is evidently unaltered by adding the same integer to j, k and l, and

$$g_{jkl} = (a_j a_k a_l)^{\frac{1}{3}} (r_j r_k r_l)^{\frac{1}{3}(2\beta-\gamma)}T_{jkl}^\beta. \tag{44}$$

It is noteworthy that the second summations in the expressions for E and V are now identical.

There remains the choice of the exponents α, β and γ. Turning to the summations in (21) and (22), we see that every term is positive. To this extent, at least, the terms combine systematically. We therefore let $\gamma = 1$. In (19) the various terms in the second summation are in general complex, and considerations of sign are insufficient to determine whether the terms cancel or not. We therefore turn to the derived equation (20), where the terms are real. Here there is little indication that the terms are mainly of one sign, and we shall assume that the behaviour is random. We therefore let $\beta = \frac{1}{2}$. Finally, we assume that the terms in the first summation in (20), each consisting of an entire second summation, combine randomly. Hence we let $\alpha = \frac{1}{2}$.

The system is now complete, assuming that the subsets $R_0, R_1, \ldots$ have been specified. It must be admitted, however, that other choices of α, β and γ might be preferable. In (22), for example, the viscous term is always negative; if a particular variable X_J is not directly forced, and if the solution has reached statistical equilibrium, positive terms must predominate over negative terms in the summations and the behaviour is not entirely random. Possibly values of α and β exceeding $\frac{1}{2}$ are indicated.

On the other hand, we may also demand that if two fields of *vorticity* are identical to one another, except that one is equal to the other 'seen through a magnifying glass' (features of equal magnitude but stretched horizontal scale), the fields should behave similarly, in the absence of forcing and viscosity. This implies that the low order equation (42) should be unaltered if j, k and l are altered by the same integer. Assuming that a_j does not increase or decrease with j, this can occur only if the factor containing $r_j r_k r_l$ in (44) drops out. The only allowable values of β and γ for which this happens are $\beta = \frac{1}{2}$ and $\gamma = 1$. Values of α exceeding $\frac{1}{2}$ still appear permissible.

4. A very low order model

In order to demonstrate that appreciable savings in computation can result from using the low order equations, we must show that it is actually possible, for some appropriate resolution factor ρ, to choose reasonably small subsets $R_0, R_1, \ldots$ of $S_0, S_1, \ldots$ while, nevertheless, retaining reasonably many interactions. We shall do this by exhibiting a particular choice.

We have noted that n_j is proportional to ρ^{2j} for large values of j. Possibly the least drastic modification which would yet offer substantial computational advantages would be one in which m_j increases less rapidly with j, perhaps as ρ^j. In the scheme which we shall present, however, m_j does not increase with j at all.

In describing the scheme it will be convenient to identify each wave vector $\mathbf{J}$ with the complex number $J_x + iJ_y$. We begin by introducing the complex numbers $z_0 = 1$ and $z_1 = 1 + i$, and, for $j \geqslant 0$, letting
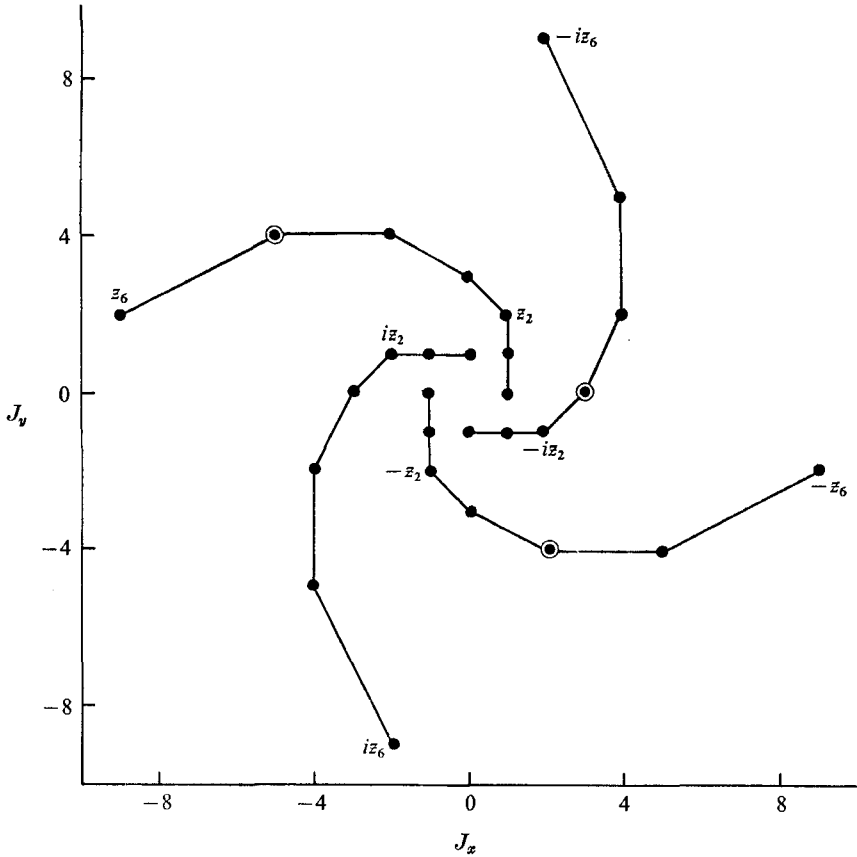
$$z_{j+2} = z_{j+1} + iz_j. \tag{45}$$

FIGURE 2. A portion of the complex plane. Points (J_x, J_y) represent complex numbers $J_x + iJ_y$. ●, $i^m Z_j$, for $j = 0, ..., 6$ and $m = 0, ..., 3$, corresponding to retained wave vectors in very low order model; ⊙, typical set of interacting vectors. Line segments connect values of Z_j, iZ_j, $-Z_j$, or $-iZ_j$ for consecutive values of j.

We then let R_j consist of the four vectors corresponding to the complex numbers $i^m z_j$, for $m = 0, ..., 3$. We shall denote the variables corresponding to z_j and iz_j by Y_j and Y'_j; those corresponding to $-z_j$ and $-iz_j$ will then be Y_j^* and $Y_j'^*$. We shall likewise denote the values of G_j corresponding to z_j and iz_j by G_j and G'_j.

Figure 2 shows the points in the complex plane corresponding to the vectors in the subsets $R_0, ..., R_6$. The points are seen to arrange themselves into four similar spirals. The points of each spiral are shown connected by line segments.

To show that there is a resolution factor ρ consistent with our choice of $R_0, R_1, ...,$ we note that the explicit solution of (45) is

$$z_j = a\lambda_1^j + b\lambda_2^j, \tag{46}$$

where λ_1 and λ_2 are the roots of the quadratic equation

$$\lambda^2 - \lambda - i = 0 \tag{47}$$

and a and b are constants chosen to make $z_0 = 1$ and $z_1 = 1 + i$. If

$$\lambda_1 = \tfrac{1}{2}[1 + (1 + 4i)^{\frac{1}{2}}] \tag{48}$$

is the root whose absolute value exceeds unity, the right-hand side of (46) is closely approximated by its first term, for larger values of j. The appropriate value of ρ is therefore

$$\rho = |\lambda_1| = \tfrac{1}{2}\{1 + \sqrt{17} + [2(1 + \sqrt{17})]^{\frac{1}{2}}\}^{\frac{1}{2}} = 1\cdot 443. \tag{49}$$

This is close to the value $\sqrt{2}$ used in constructing figure 1. Since half-octave resolution is very convenient, we shall make a further approximation by letting $\rho = \sqrt{2}$ when computing the coefficients in (42).

It is evident from (45) that for any value of j the vectors corresponding to the numbers z_{j+2}, $-z_{j+1}$ and $-iz_j$ interact, as do the vectors corresponding to the products of these numbers with i, -1 or $-i$. From figure 2 it appears that there are also four interactions each involving two vectors in R_0 and one in R_1, but we shall omit these from our system, whereupon all the retained interactions are among vectors in three consecutive bands. This is precisely the situation illustrated in figure 1.

If now $k = j + 1$ and $l = j + 2$, it follows that $p_{jkl} = 4$ for all values of j. By definition of the subsets, $m_j = 4$. Hence $\rho_{jkl} = \tfrac{1}{4}$. The values of q_{jkl} and n_j and hence σ_{jkl} may easily be found by a direct count, even for rather large values of j if a fast enough computer is used. We find that σ_{jkl} approaches a limit of about $0\cdot 19$ as $j \to \infty$, and we shall use this value for all values of j. Thus $\tau_{jkl} = 0\cdot 76$. As we noted in discussing figure 1, a reasonably satisfactory choice for a_j for large values of j is $(7\cdot 1)^\alpha = 2\cdot 67$, and we shall use this value for all j. It follows that $q_{jkl} = 2\cdot 34$.

Again for $k = j + 1$ and $l = j + 2$, it follows from (43) and (10) that $C'_{jkl} = \tfrac{1}{16}\sqrt{7}$, while $C'_{klj} = -3C'_{jkl}$ and $C'_{ljk} = 2C'_{jkl}$. Finally, if **J**, **K**, and **L** are any interacting vectors in R_j, R_k and R_l, $\epsilon_{\mathbf{JKL}} = +1$. Assembling these results, we find that the governing equation (42) may be written as

$$\frac{d}{dt}Y_j = c(2Y'_{j-2}Y_{j-1} - 3\,Y'^{*}_{j-1}Y_{j+1} + Y'_{j+1}Y'^{*}_{j+2}) - 2^j\nu D^{-2}Y_j + G_j, \tag{50}$$

$$\frac{d}{dt}Y'_j = c(2\,Y^{*}_{j-2}Y'_{j-1} - 3Y_{j-1}Y'_{j+1} + Y^{*}_{j+2}Y_{j+2}) - 2^j\nu D^{-2}Y'_j + G'_j, \tag{51}$$

where a reasonably suitable value for c is $\tfrac{3}{4}$, if $\alpha = \tfrac{1}{2}$. An otherwise unneeded factor of 2 enters c because the sums in (50) and (51) are not redundant. It is to be understood that Y_j and Y'_j vanish if $j < 0$.

We close this demonstration with a non-trivial special case of (50) and (51) which is even simpler than the general case. Suppose that, for each j, G_j and G'_j are real and equal, while Y_j and Y'_j are real and equal initially. In this event Y_j and Y'_j remain real and equal. Physically this restriction implies that the flow pattern, which is already periodic in x and y, is left unaltered by a rotation about the origin through a right angle.

For this case alone it is convenient to let $y_j = 2Y_j$ and $g_j = 2G_j$. The behaviour

in the jth band is now represented by the single real variable y_j, and E and V are now given by

$$E = \tfrac{1}{2}D^2 \sum_{j=0}^{\infty} 2^{-j}y_j^2, \tag{52}$$

$$V = \frac{1}{2}\sum_{j=0}^{\infty} y_j^2, \tag{53}$$

while (50) and (51) reduce to

$$\frac{d}{dt}y_j = c_0(2y_{j-2}y_{j-1} - 3y_{j-1}y_{j+1} + y_{j+1}y_{j+2}) - 2^j\nu D^{-2}y_j + g_j, \tag{54}$$

where $c_0 = \tfrac{1}{2}c$ may be taken as $\tfrac{3}{8}$. To solve (54) numerically we must further truncate the system by letting $y_j = 0$ when j exceeds some integer N, but E and V are still conserved by each interaction.

5. Comparison with an accurate numerical simulation

In order to gain some idea as to the adequacy of the low order models, we shall compare some numerical solutions of the very low order equations with more conventional numerical simulations of turbulence. The solution which we have chosen for comparison represents decaying two-dimensional turbulence, and was obtained by Fox (1972). The computational procedure, proposed by Orszag (1971), involves representing the field of motion in wavenumber space, retaining all components of scalar wavenumber less than 32, and also in physical space, using a grid of 64×64 points. Within each time step the linear operations, including inversion of ∇^2, are performed in wavenumber space, while the multiplications are performed in physical space. Between these operations one transforms back and forth from one space to the other, using fast Fourier transform procedures.

The particular numerical simulation which we shall attempt to reproduce uses a relatively large viscosity $\nu D^{-2} = 0\cdot01$ units, and is considered 'accurate' in the sense that the statistical properties of the solution are not affected by the truncation at a wavenumber of 32. That is, the bulk of the enstrophy dissipation occurs at wavenumbers considerably less than 32 and, presumably, if still higher wavenumbers had been retained, the corresponding variables would have remained so close to zero that any interactions involving them would not have significantly affected the lower wavenumbers.

To facilitate the comparison we have redrawn Fox's spectra with an ordinate of mean-square vorticity per half octave (on a logarithmic scale). Figure 3 shows his spectra at $t = 0$ and also at $t = 2\cdot32$, the time which he chose for discussion. Also shown is the spectrum which would have resulted at $t = 2\cdot32$ if the nonlinear terms had been absent; we shall call this the *linear-decay* spectrum. The difference between the spectra at $t = 2\cdot32$ represents the cumulative influence of the nonlinear processes, which clearly is a transfer of enstrophy from the intermediate scales, which initially contain the bulk of the enstrophy, to the larger and smaller scales.

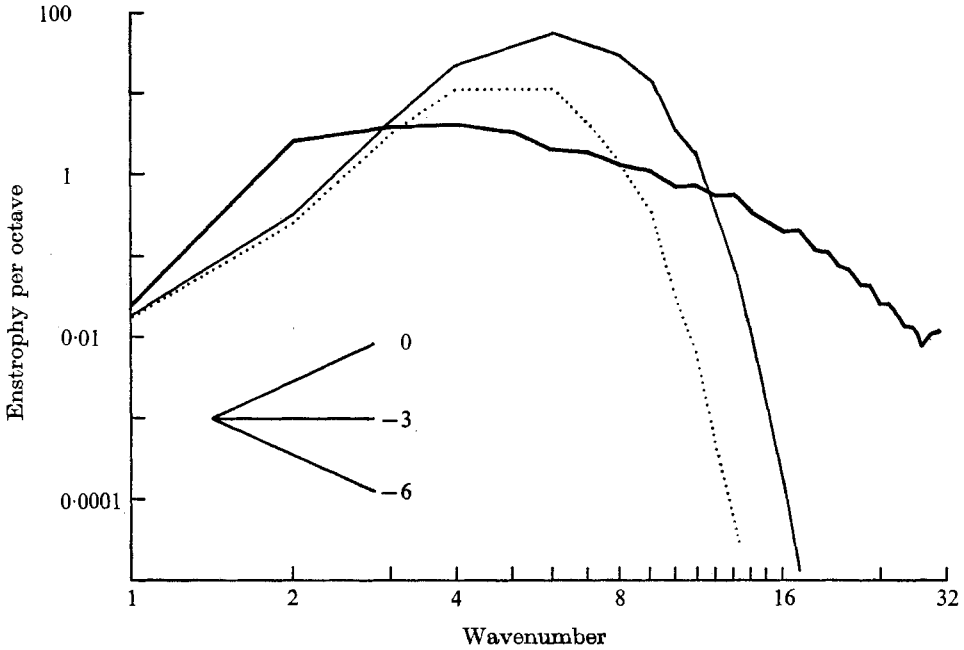In our attempt to reproduce these results with the very low order model, we

FIGURE 3. Initial spectrum (thin solid curve), spectrum at $t = 2\cdot32$ (heavy solid curve) and linear-decay spectrum at $t = 2\cdot32$ (dotted curve) in numerical simulation of decaying turbulence by Fox (1972). Segments labelled 0, -3, and -6 indicate slopes which curve would have if energy per wavenumber varied as 0, -3 and -6 power, respectively, of the wavenumber.

t	y_0	y_1	y_2	y_3	y_4	y_5	y_6	y_7	y_8	y_9	y_{10}
0·00	0·13	0·27	0·56	1·72	4·68	6·68	5·31	1·00	0·01	0·00	0·000
0·48	0·24	0·61	1·81	1·00	4·63	−1·24	4·91	0·31	2·21	0·51	0·093
0·96	0·34	−0·15	1·62	−2·70	−0·89	−4·73	−2·18	−0·26	0·63	−0·10	−0·003
1·44	0·18	−0·61	1·65	1·66	−3·16	−2·70	2·49	−0·45	0·16	0·00	0·000
1·92	0·09	0·02	1·44	3·11	0·67	−2·09	1·67	−1·39	−0·51	0·06	−0·001
2·40	0·19	0·48	1·88	0·38	3·34	−0·66	−0·61	−0·87	−0·18	0·05	−0·001
2·88	0·27	−0·10	1·38	−2·41	2·30	−0·45	−0·83	−0·41	0·04	0·00	0·000

TABLE 1. Particular solution of the very low order equations, with $\nu D^{-2} = 0\cdot01$ and no external forcing

have used eleven variables $y_0, \ldots, y_{10}$, representing wavenumbers from 1 to 32. The initial values of y_j^2 were simply read from the initial-state spectrum; this gave initial values of 1·86 and 49·5 for E and V, as compared to Fox's values of 1·81 and 50·1. In our first experiment the initial values of y_j were the *positive* square-roots of y_j^2. For time differencing we used the 4-cycle form of the N-cycle scheme recently presented by the writer (1971a). The basic time increment Δt was chosen as 0·12, after some experimentation showed that reducing Δt to smaller values did not appreciably affect the results. Table 1 shows the values of the eleven variables at intervals of four time steps, up to the 24th step.
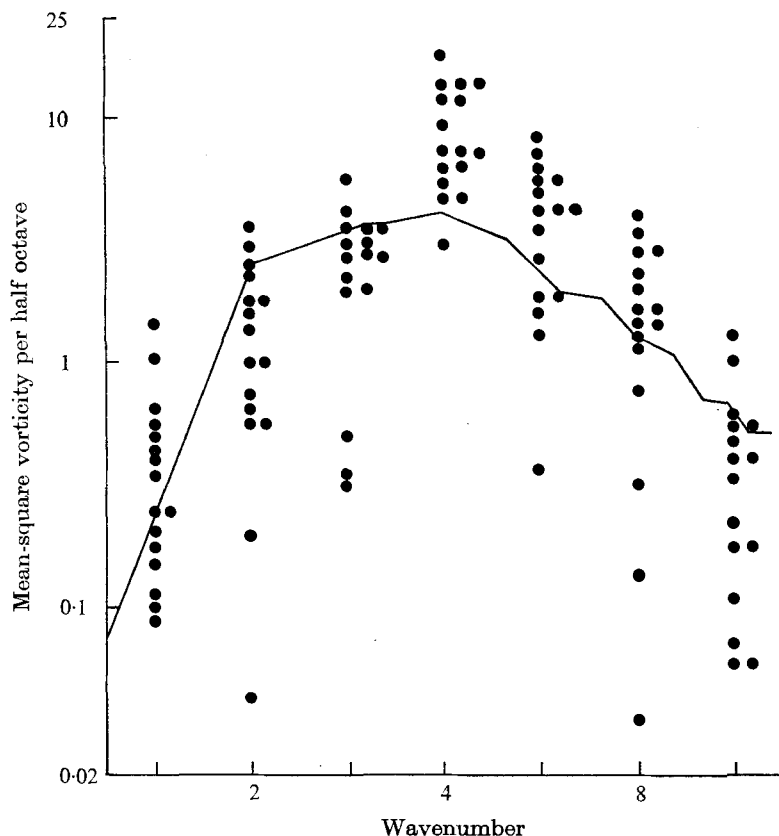
FIGURE 4. Mean-square vorticity per half octave averaged from $t = 1.92$ to $t = 2.76$ (solid circles), obtained from 16 different solutions of the very low order equations with $c_0 = \frac{3}{8}$, compared with spectrum at $t = 2.32$ (solid curve) taken from figure 3.

The squares of the values of y_j at $t = 2.40$ might be considered a first attempt to reproduce the accurate spectrum for $t = 2.32$. While there is some order-of-magnitude agreement, the variation of y_j^2 with j is obviously far too erratic. This behaviour is to be expected in a model where one variable must singly represent the behaviour of many components. In general the variables y_j change sign as time evolves, and it is likely that at any particular time some variables will be near their zero crossings, while others will be near their peaks. Thus the value $y_3^2 = 0.14$ at $t = 2.40$ falls far short of the appropriate value of 3.5 indicated in figure 3, while the value $y_4^2 = 11.2$ exceeds the proper value of 4.0. To some extent we can reduce this difficulty by averaging y_j^2 over several successive time steps, but to perform a proper simulation with the very low order model we should work with a collection of solutions.

Accordingly we have determined 16 solutions of (54). The initial values of y_j^2, and hence the initial spectrum, are the same in all cases, while the initial values of y_j form 16 different arrangements of positive and negative square-roots of y_j^2. For each solution we have averaged the values of y_j^2 from the sixteenth to the twenty-third time step; the central time is therefore $t = 2.34$. Figure 4 shows the
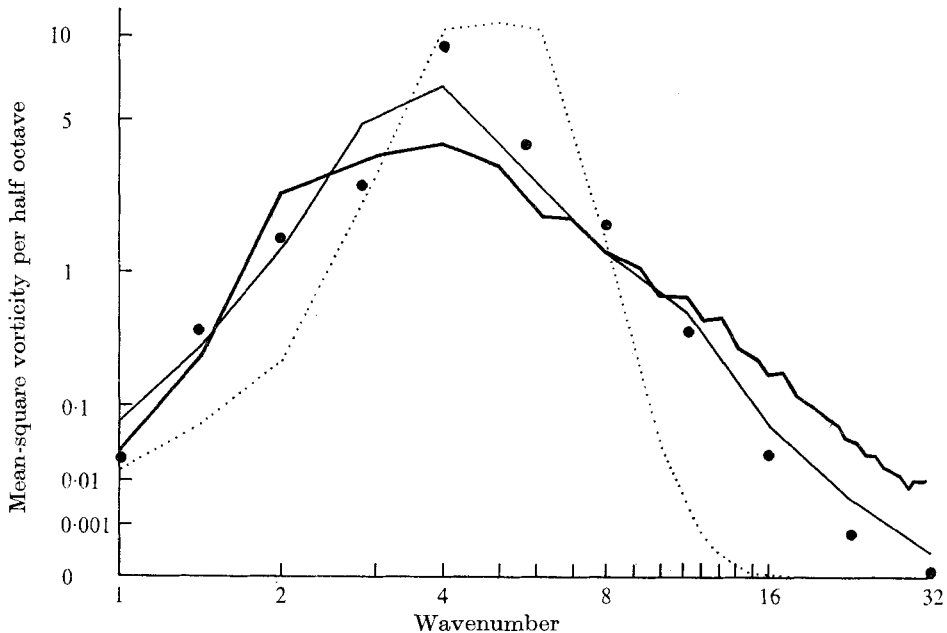
FIGURE 5. Spectrum averaged from $t = 1.92$ to $t = 2.76$ and averaged over 16 solutions of the very low order equations with $c_0 = \frac{3}{8}$ (solid circles), and spectrum averaged from $t = 1.92$ to $t = 2.80$ and averaged over 16 solutions of the very low order equations with $c_0 = \frac{3}{4}$ (thin solid curve), compared with spectrum at $t = 2.32$ (heavy solid curve) and linear-decay spectrum at $t = 2.32$ (dotted curve) taken from figure 3.

16 average values of y_j^2 so obtained, for $j = 1, ..., 7$, and also the accurate spectrum at $t = 2.32$ for comparison. There is great variation from one solution to another, in some instances by a factor of 100. Nevertheless, any reasonable method of averaging the 16 solutions together would produce a spectrum, over the wavenumbers appearing in figure 4, showing general agreement with the accurate spectrum, although with too strong a peak at a wavenumber of 4.

The arithmetic average of the 16 spectra is represented by the solid circles in figure 5, where it is compared with the accurate spectrum and the linear-decay spectrum at $t = 2.32$, taken from figure 3 (and drawn on a fourth-root instead of a logarithmic scale to facilitate comparison over all wavenumbers). It is evident that the very low order model has captured the effects of the nonlinear processes, qualitatively. Nearly all the circles lie on the proper side of the linear-decay spectrum. However, there are obvious quantitative shortcomings. In general the nonlinear effects are underestimated; it is as if the circles were an interpolation between the linear-decay spectrum and the accurate spectrum.

The principal failing is at the small scales, where our spectrum is too low by a factor of nearly 10 at a wavenumber of 16 and nearly 100 at a wavenumber of 22. This failing is readily accounted for, however, and could have been anticipated.

In the accurate solution, when $t = 2.32$, the enstrophy in the high wavenumbers is decreasing only slowly with time, the rapid viscous decay being nearly, but not quite, balanced by the nonlinear transfer of enstrophy from lower wavenumbers. In the very low order model (but not in the general low order model) the nonlinear

interactions are all local in wavenumber space; that is, they involve only adjacent scales. In particular, the only nonlinear term in (54) affecting y_{10} is $2c_0 y_8 y_9$. It is evident that if y_8, y_9 and y_{10} temporarily assumed orders of magnitude demanded by the accurate solution, say $y_8 = 0.4$, $y_9 = 0.2$ and $y_{10} = 0.1$, the gain in enstrophy in the smallest scale, namely $2c_0 y_8 y_9 y_{10} = 0.006$, would be far less than the dissipation of enstrophy, $2^{10}\nu D^{-2} y_{10}^2 = 0.1$, and the proper magnitude would not persist. Similar considerations apply to the maintenance of enstrophy in scales 8 and 9, although the imbalance is less extreme. It follows also from similar reasoning that in the accurate solution the enstrophy dissipation in the smallest scales must be balanced mainly by interactions which are not local in wavenumber space. Hence a model in which all the interactions are local will not produce an adequate spectrum in scales at the high wavenumber end of the dissipation range.

At some of the remaining wavenumbers the discrepancy between our spectrum and the accurate spectrum is insignificant, but it is especially noticeable at scale 4, where it exceeds a factor of two. The general conclusion is that the nonlinear effects in the very low order model are qualitatively correct, but not strong enough.

The immediate suggestion is that we might improve the model by intensifying the nonlinear effects. One obvious procedure which might accomplish this end would be to use a larger constant c_0. We can justify such a change by noting that the constant α in (37), which we took to be $\frac{1}{2}$, could be increased on the grounds that the effects of the separate triples of scales containing interactions may combine more or less systematically, even though the separate interactions within a triple do not.

Accordingly, we have doubled the value of c_0, to $\frac{3}{4}$, which corresponds to $\alpha = 0.85$, and we have obtained 16 more solutions, using the same 16 sets of initial conditions as before, but reducing the time increment Δt to 0.06 to avoid excess computational error. The spectrum averaged over time steps 32 to 47 (average time $t = 2.37$) and over all 16 solutions appears in figure 5 as the thin solid curve. We see that there is appreciable improvement at nearly every scale, but that perfection is yet to be reached. At the smallest scales, where the improvement is greatest, the room for further improvement is also greatest. For good measure we also obtained 16 solutions with $c_0 = 1$, which corresponds approximately to $\alpha = 1$, the largest allowable value. There was no appreciable difference between these results and those obtained with $c_0 = \frac{3}{4}$.

We conclude that the very low order model is capable of yielding a qualitatively correct representation of the nonlinear effects. Quantitatively the effects are fairly well represented, although somewhat underestimated, except in scales at the high wavenumber end of the dissipation range, where the very low order model, or any other model in which the interactions are local in wavenumber space, is incapable if producing an accurate spectrum.

6. Concluding remarks

Even though the low order equations entail a considerable number of approximations, they nevertheless retain some of the features of the equations governing two-dimensional turbulence. Like the latter equations, the former describe the

behaviour of a collection of nonlinearly coupled dependent variables, and these variables represent features of widely differing scales.

The identification of the separate variables with separate scales of motion is not just a matter of labelling. First of all, the smaller scales are subject to much greater viscous dissipation than the larger ones. More important, however, the coefficients in the nonlinear terms are such that in the absence of external forcing and viscous dissipation the equations possess two distinct quadratic invariants, representing kinetic energy and enstrophy, with the larger scales contributing much more heavily to the kinetic energy than to the enstrophy, while the opposite is true for the smaller scales.

It may therefore be anticipated that individual solutions of the low order equations will exhibit many of the properties of two-dimensional turbulence, although certainly not all. The very low order equations, whose solutions we compared with a more conventional numerical simulation, appear capable of producing reasonably accurate spectra of decaying turbulence, except at rather high wavenumbers.

Meanwhile, restricted collections of vectors possessing reasonably many interactions are not limited to the one used in the very low order model, and the advantages of less drastic simplifications should be considered. One shortcoming of the very low order model was seen to be the local character of the interactions. The equations cannot describe such processes as the conveyance of small-scale details by large-scale currents. Another perhaps equally serious fault is that the model effectively leaves too many tasks to be accomplished by too few variables.

As a first step in remedying this situation we might, for example, let the subset R_j contain the four vectors corresponding to $i^m z_j$, defined as in the very low order model, and the additional four vectors $i^m w_j$, where $w_j = (1+i) z_{j-1}$. The vectors then form eight spirals in wave-vector space, and it is easily verified that whereas there are twice as many variables as in the very low order model, there are five times as many interactions, some of which are less local. The retention of still more vectors might further improve the situation.

It remains to be seen whether low order models containing some non-local interactions can produce correct spectra even at very small scales, and whether any low order models can produce reasonable spectra of developing or stationary turbulence as well as decaying turbulence. Nevertheless, our experience with the very low order model must be considered encouraging.

REFERENCES

Fox, D. G. 1972 Numerical procedures for studying incompressible two-dimensional turbulence. *A.I.A.A. 10th Aerospace Sciences Meeting (San Diego), Paper* no. 72–152.

Kraichnan, R. H. 1959 The structure of isotropic turbulence at very high Reynolds numbers. *J. Fluid Mech.* **5**, 497–543.

Lilly, D. L. 1969 Numerical simulation of two-dimensional turbulence. *Phys. Fluids*, **12** (suppl. 2), 240–249.

Lorenz, E. N. 1971a An N-cycle time-differencing scheme for stepwise numerical integration. *Mon. Weather Rev.* **99**, 644–648.

Lorenz, E. N. 1971b Investigating the predictability of turbulent motion. *Proc. Sympos. Statistical Models and Turbulence. Lecture Notes in Physics*, vol. 12, pp. 195–204. Springer.

Millionshtchikov, M. D. 1941 On the theory of homogeneous isotropic turbulence. *C.R. Acad. Sci. U.R.S.S.* **32**, 615–618.

Ogura, Y. 1963 A consequence of the zero-fourth-cumulant approximation in the decay of isotropic turbulence. *J. Fluid Mech.* **16**, 33–40.

Orszag, S. A. 1970 Analytical theories of turbulence. *J. Fluid Mech.* **41**, 363–386.

Orszag, S. A. 1971 Numerical simulation of incompressible flows within simple boundaries: accuracy. *J. Fluid Mech.* **49**, 75–112.